FINAL TECHNICAL REPORT FOR GRANT NUMBER: G13AP00072

EXPERIMENTS TO UNDERSTAND DYNAMIC FRICTION DURING EARTHQUAKES

Terry E. Tullis
Tele: (401) 863-3829
FAX: (401) 863-2058
Email: Terry_Tullis@brown.edu

and

David L. Goldsby
Tele: (401) 863-1922
FAX: (401) 863-2058
Email: David_Goldsby@brown.edu

both at

Brown University
Department of Geological Sciences
Providence RI 02912-1846

Note: As of July 1, 2014 David L. Goldsby moved from Brown.
His current contact information is:
Tele: (215) 746-0090
Email: dgoldsby@sas.upenn.edu

Department of Earth and Environmental Sciences
University of Pennsylvania
160 Hayden Hall
240 South 33rd Street
Philadelphia, PA 19104-6316

September 1, 2013 to April 30, 2015

ABSTRACT

In order to determine where best to deploy limited resources for mitigating earthquake loss in the US, we need to understand when and where earthquakes may occur and how intense their accelerations can be. Every time an earthquake occurs, we gain more understanding of the earthquake problem through measurements of ground-motion and modeling of seismic sources. In addition to information derived from earthquakes, we also benefit from improved understanding of the seismic source through laboratory measurements and modeling to anticipate phenomena that may occur in future earthquakes. One of the great gaps in our understanding of source processes is how shear resistance varies on a fault during rapid coseismic slip and what this implies about the magnitudes of stress drops and near-fault accelerations. We are helping to fill that gap through our laboratory experiments.

During recent years we have conducted research to understand three potential dynamic fault-weakening mechanisms: silica gel weakening, flash heating, and thermal pore-fluid pressurization. We report this year on our most recent achievements in producing thermal pore-fluid pressurization. Although others have also shown weakening in the lab due to this mechanism, we are alone in possessing the unique experimental capabilities and experience gained in the last few years to quantitatively study this mechanism in the laboratory. Our high-pressure rotary-shear apparatus is the only machine in existence that combines arbitrarily large slip displacement with independent control of both confining pressure and pore pressure. In other words, ours is the first study in which this mechanism has been isolated and is beginning to be characterized under controlled conditions on confined samples (e.g., with fully saturated rocks of controlled fluid pressure and proscribed permeabilities of the rock samples).

We have developed a successful protocol for thermally cracking our initially low permeability Frederick diabase samples ($<10^{-23}$ m^2) and measuring the resulting permeabilities in the 10^{-23} m^2 to 10^{-18} m^2 range. As demonstrated herein, during 2013-15 we have conducted experiments on bare surfaces of Frederick Diabase that clearly demonstrate the operation of dynamic weakening due to thermal pressurization; we have measured the temperature near the sliding surface with a thermocouple embedded in the sample in the presence of elevated pore pressure, and we have used finite element model (FEM) calculations of the temperatures achieved in our experiments to understand the temperature evolution in time and space. Furthermore, we have recently merged FEM analysis of fluid diffusion with our analysis of thermal diffusion to understand the pore-pressure evolution during the experiment in time and space. We have written a paper that is nearly ready to be submitted for publication in *Nature* describing our experimental results and how they compare with theoretical predictions; some of the results in that paper are presented here.

Our experience gained over the last three years in studying thermal pressurization shows that the permeability in our thermally cracked diabase is a strong function of effective confining pressure. Looking ahead, we plan to add this dependency in our FEM models of fluid diffusivity which should allow us to make more accurate models of our samples that will demonstrate how well the experiments and theory agree. We also plan to investigate the role that slip-induced dilatancy due to fault roughness may play in defeating the increase in pore fluid pressure due to thermal pressurization. When this is completed we will have quantified the effects of sliding velocity, sliding displacement, normal stress, fluid pressure, and dilatancy on the operation of this high-speed weakening mechanism. Thus we should be able to draw a conclusion concerning the importance of thermal pressurization for causing high-speed weakening on natural faults.

Constitutive equations for thermal pressurization are being employed in dynamic-rupture models; it is imperative that we better understand the underlying physics of this mechanism. At present the only other experimental data that bear on this mechanism are qualitative. Through our continuing study of thermal pressurization, we are gaining understanding of how the shear resistance on faults varies during earthquakes and what the observed behavior implies for earthquake rupture and strong ground-motion.

INTRODUCTION

During past years, we have been investigating the frictional properties of rocks at seismic slip rates. Our experiments to date have addressed three distinct weakening mechanisms that occur at sliding velocities above ~1 mm/s. First, a previously unknown mechanism, silica-gel weakening, operates above velocities of ~1 mm/s and requires hundreds of mm of slip to be activated [*Di Toro et al.*, 2004; *Goldsby and Tullis*, 2002]. Second, flash weakening of asperity contacts operates above ~0.1 m/s (for many crustal silicate rocks) and requires only fractions of a mm of slip to be effective [*Beeler et al.*, 2008; *Goldsby and Tullis*, 2011; *Kohli et al.*, 2011; *Rice*, 2006].

Third, although further research investigating the details of these mechanisms and their applicability to earthquakes is warranted, we have turned our attention to the widely discussed mechanism of weakening due to thermal pressurization of pore fluids. In spite of the fact that there are many theoretical and numerical studies of this weakening mechanism [*Andrews*, 2002; *Lachenbruch*, 1980; *Lee and Delaney*, 1987; *Mase and Smith*, 1985; 1987; *Noda*, 2008; *Noda and Shimamoto*, 2005; *Rempel and Rice*, 2006; *Rice*, 2006; *Rice and Cocco*, 2007; *Sibson*, 1973] and it is increasingly used in dynamic rupture and earthquake nucleation models [*Bizzarri and Cocco*, 2006a; b; *Lapusta and Rice*, 2004a; b; *Noda et al.*, 2009; *Noda and Lapusta*, 2010; 2012; *Rice et al.*, 2010; *Schmitt and Segall*, 2009; *Segall and Rice*, 2006], there are no experimental studies that quantitatively demonstrate the operation of this process, although [*Faulkner et al.*, 2011] and [*Ujiie et al.*, 2013] have some rather convincing evidence that thermal pressurization played a role in the weakening in their unconfined high-speed rotary shear samples. Consequently, it is important to determine if its occurrence can be better understood and if its relevance for earthquakes can be evaluated. Below we describe our progress in conducting experiments on this difficult-to-study weakening mechanism and then proceed to describe the work we plan to do next on this topic.

Thermal pressurization experiments are being conducted on bare surfaces of fine-grained Fredrick diabase that we collected from the classic area of its original sampling in Maryland [*Adams and Gibson*, 1929], as well as simulated gouges (comprised of diabase or other materials). Diabase is used because it does not undergo gel weakening at large slip displacements and high slip rates as do other silicate rocks of higher silica content [*Roig Silva et al.*, 2004a; b], and it does not weaken due to flash heating at the modest (sub-0.1 m/s) slip rates of our experiments [*Goldsby and Tullis*, 2011]. Thus any observed weakening due to thermal pore-fluid pressurization will not be convolved with that due to other known dynamic weakening mechanisms. This expectation has been borne out by our experiments to date. A further advantage of this rock is that in its original state its permeability is so low (less than 10^{-23} m/s^2 according to our measurements) that it is impractical to saturate it in reasonable laboratory times. However, by subjecting the diabase to a thermal treatment at a variety of temperatures it is possible to create higher permeabilities, and in this way we have been able to control the permeability over the range from 10^{-23} to 10^{-18} m^2. Because permeability is a critical parameter for thermal pressurization, we can compare experimental results with theoretical predictions for the rate of weakening with slip as a function of slip velocity and permeability.

The experiments within the past two years demonstrate that thermal pressurization occurs at a range of permeabilities and slip rates and that we are able to understand the results quantitatively with a combination of analytical and finite element models (FEM).

Background/Overview of recent progress

Within the past two years, we have made important progress in our understanding of the dynamic fault-weakening mechanism termed thermal pore-fluid pressurization. Thermal pressurization is simple in concept – for sufficiently low permeabilities of fluid-saturated fault zones, severe frictional heating during earthquake slip causes trapped pore fluids to thermally expand, increasing the pore-fluid pressure, thereby decreasing the effective normal stress and hence the dynamic shear stress. Although theoretical models of this physical process exist, prior to our work no experimental results exist which corroborate and test existing theories quantitatively. We continue to conduct thermal pressurization experiments using Frederick diabase and by thermally cracking it (based on previous thermal cracking studies of this rock [*Fredrich and Wong, 1986*]) we systematically vary the permeability of the samples over a critical range of low values. Permeability as well as fault normal dilation or compaction are first-order factors in determining whether fault zones (and our experimental samples) become pressurized due to frictional heating of trapped fluids. During the past year we have come to realize that not only the fluid diffusivity of our samples but also their thermal diffusivity is changed somewhat by the thermal cracking, and this has allowed us to make more sense of our results.

Within the past year, we have conducted new high-speed friction experiments on bare surfaces of diabase to study thermal pressurization. We have also conducted new finite element modeling (FEM) in which we have added fluid diffusion to the analysis of thermal diffusion begun in previous years. The combination of our new experiments with our new FEM analysis that shows the spatial and temporal variation of the temperature and pore pressure distribution in our samples, has allowed us to come to a better understanding of the behavior of our experiments and of the process of thermal pressurization, although some puzzles remain in the details.

Theoretical background on dynamic weakening by thermal fluid pressurization

Although there are many theoretical studies of the thermal pressurization weakening mechanism, as cited in the introduction, we will focus our discussion on the most recent and comprehensive one, that of *Rice* [2006]. Rice presents solutions for many situations, but the one relevant to our experiments is his slip-on-a-plane solution for fault slip on the boundary of a half-space. His equations 23a and B19 show that at constant slip velocity V, the shear stress τ decays with slip distance δ as follows:

$$\tau(\delta) = \mu(\sigma_n - p) = \mu(\sigma_n - p_0)\exp\left(\frac{\delta}{L^*}\right) erf\left(\sqrt{\frac{\delta}{L^*}}\right) , \qquad (1)$$

where μ is the coefficient of friction, σ_n is the normal stress, p is the current pore pressure, p_o is the initial pore pressure, and L^* is a decay distance given by *Rice* [2006, equation 23b] as

$$L^* = \frac{4}{\mu^2 V}\left(\frac{\rho c}{\Lambda}\right)^2 \left(\sqrt{\alpha_{hy}} + \sqrt{\alpha_{th}}\right)^2 , \qquad (2)$$

where ρc is the density times the heat capacity, Λ is his undrained pressurization factor, and α_{hy} and α_{th} are the hydraulic and thermal diffusivities, respectively. Below we will show how the observed decay of shear stress in our experiments follow a decay of the form given by (1) with a decay distance L^* that varies between experiments in a way that is consistent with equation (2).

However, before we can make this comparison we must address an important difference between the half-space assumed by *Rice* [2006] and the geometry of our sample assembly. The steel sample grips, into which our samples are epoxied, are relatively close to the sliding fault surface. Thus the temperature of the sample cannot continue to rise as fast as in the half space case as soon as enough time has elapsed that the heat has diffused as far as the steel. This complexity has required that we create a finite element model (FEM) of our sample assembly in order to quantitatively understand the temporal and spatial history of temperature and pore pressure in our samples. However, we would still expect that for a few seconds, before the heat diffuses as far as the steel sample grips, the initial part of the decay in shear stress would be predicted by (1).

Experiments

Procedures – Our rapid-sliding experiments have been conducted on initially bare surfaces of Frederick Diabase. The bare-surface diabase samples were thermally cracked [*Fredrich and Wong*, 1986] via temperature excursions in the range 725 ^{o}C to 806 ^{o}C, at a ramp rate of ~400 ^{o}C/hr. The resulting permeability depends on the treatment temperature.

Experiments were conducted on samples fully saturated before frictional sliding. Because of the low permeability of the diabase rings, a relatively high pore pressure must be applied to the samples to saturate them in a practical amount of time. Saturation thus had to be accomplished with the samples subjected to relatively large pore pressures while confined in the high-pressure apparatus. The following procedure was therefore developed: 1) samples were pressurized in the gas apparatus, 2) a constant pore pressure was applied to the lower sample grip, 3) pore pressure was held constant until water could be seen exiting the sample assembly from the pore-pressure tubing connected to the upper sample ring, 4) the sample was depressurized and the pore-pressure port on the bottom sample grip was plugged (the flow-through tubing used during saturation is incompatible with the large sliding displacements, sometimes meters of slip, of our thermal pressurization tests), 5) the sample was repressurized to the testing temperature and the desired pore pressure of the run conditions was applied, and 6) sliding was commenced after the externally applied pore pressure was equilibrated throughout the sample (i.e., after no movement of the pore pressure piston into the pore pressure cylinder was observed). Due to the low permeability of the sample, fluid pressure within the fault zone may deviate significantly from the applied value when fluid pressure changes rapidly on the fault.

Thermal pressurization weakening results

Results for several experiments are shown in Figures 1-3. The experimental results in Figure 1 for experiment 312pfp we showed in last year's report, but the fit to *Rice's* [2006] analysis had not yet been made. Figure 1 shows the portion of the experiment immediately after the slip rate was increased from 10 μm/s to 4.8 mm/s. The shear stress decreases by 20%, within the first 6 s (28 mm of slip). A fit made by John Platt to equation (1) shows a good fit to the form of the falloff with a value of $L^* = 500$ mm. This sample had a permeability of $6.1*10^{-19}$ m^2.

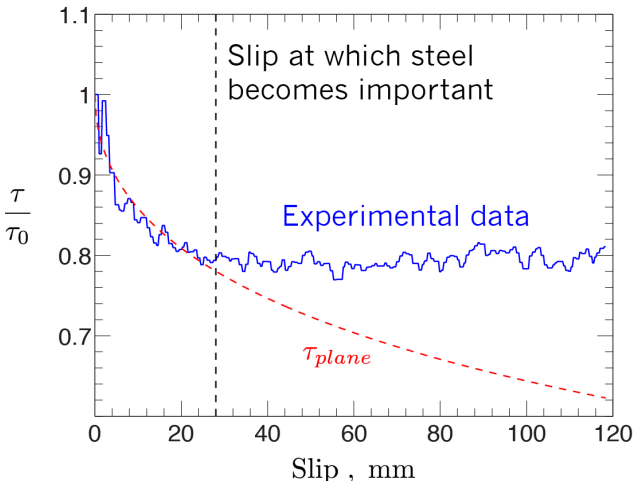

Figure 1. Fit to L* of equation (1) for experiment 312pfp at 4.8 mm/s. Red curve is for half space with $L^* = 500$ mm.

For another experiment, 319pfp, Figure 2 shows similar decays and fits to equation (1) with values of L* of 4800 mm for v=1.2 mm/s, 2400 mm for V=2.4 mm/s, and 1200 mm for V=4.8 mm/s. Note that the drop in shear stress is 5% at 1.2 mm/s, 10% at 2.4 mm/s and 20% at 4.8 mm/s. This sample was more permeable than 312pfp with a value of $1.3*10^{-18}$ m^2.

Figure 3 shows data and a fit to equation (1) for experiment 329pfp at a slip rate of 2.5 mm/s. Note the much more significant decrease in the shear stress when the velocity was stepped from 1 μm/s to 2.5 mm/s, a drop of 80%,. This sample had a permeability of $1.6 *10^{-20}$ mm^2 so it was considerably less permeable than the other samples, 38 times lower than those for 312pfp and 81 times smaller than for 319pfp. This presumably explains the large stress reduction. Figure 3b shows that the form of the decay does not fit the form of equation (1) as well as do the decays in experiments 312pfp and 319pfp. The value of L^* for the fit shown by the

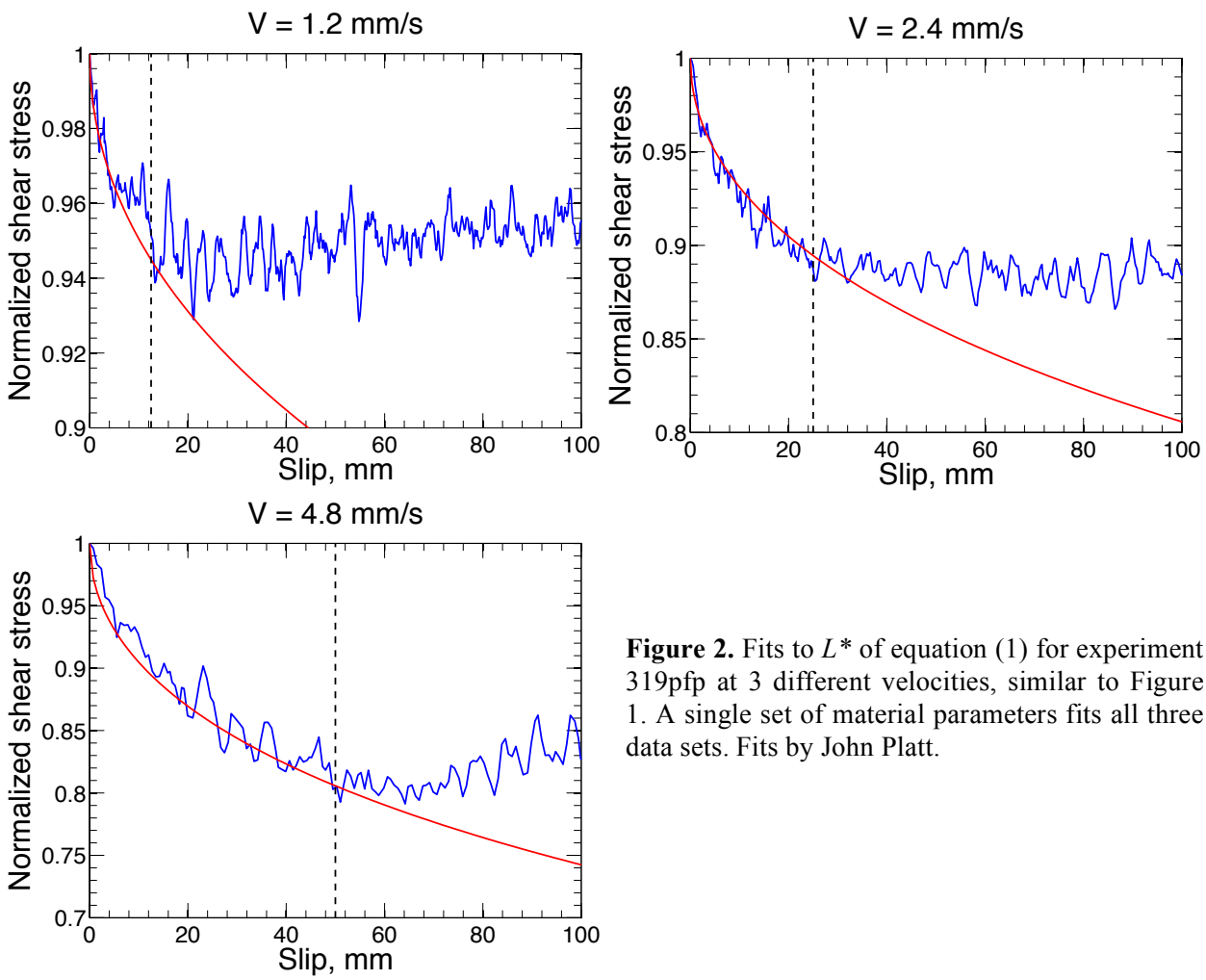

Figure 2. Fits to L^* of equation (1) for experiment 319pfp at 3 different velocities, similar to Figure 1. A single set of material parameters fits all three data sets. Fits by John Platt.

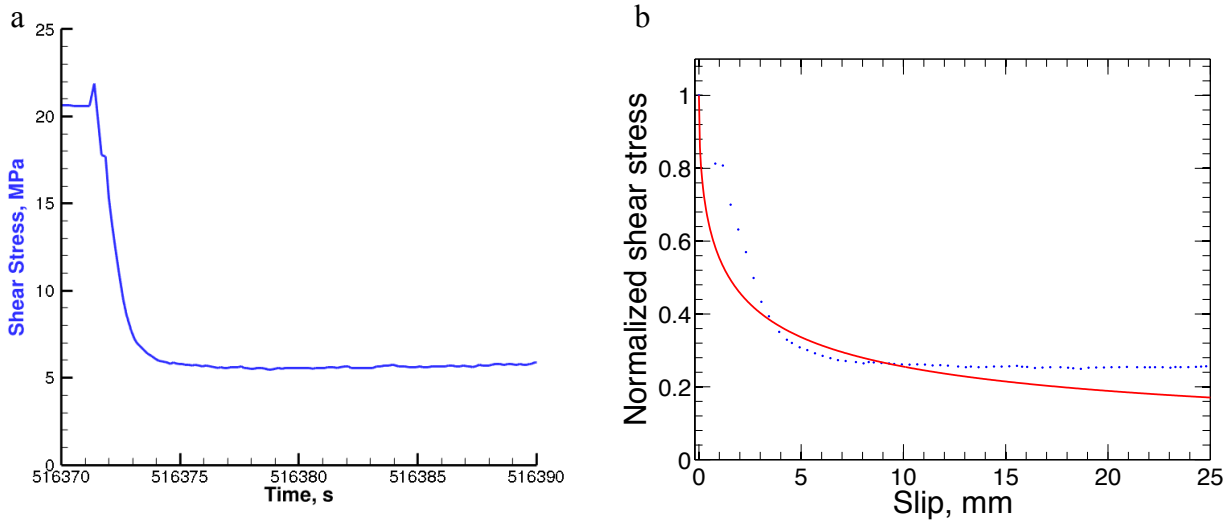

Figure 3. Data in blue **o**n left and in dots on right for experiment 329pfp for a step from 1 μm/s to 2.5 mm/s. Red curve is best fit to equation (1) found by John Platt with $L^* = 2.5$ mm.

red line is 2.5 mm. Although the shear stress drop of 21.5 MPa shown in Figure 3a suggests that the pore pressure rose almost to the confining pressure of 25 MPa (the friction coefficient is in the 0.85 to 0.9 range), the drop does not seem to result from a jacket leak because the confining pressure was not changed at this time and its servoed pumping system did not turn on.

Several lines of evidence strongly indicate that the weakening shown in Figures 1-3 is due to thermal pressurization. One of these is that the form of the decay nicely matches the theoretical expectations from *Rice's* [2006] analysis presented here as equation (1). We do not understand the reason for the poorer quality of the fit for experiment 329pfp although it may be a result of the hydraulic properties changing as a function of the effective pressure as we discuss in a section below. Note that this sample is the one for which the effective pressure within the sample changed the most, so it would be expected to have the greatest change in parameter values.

An important point arguing that the weakening shown in Figure 2 is due to thermal weakening is that the three values of L^* follow the theoretical dependence of L^* on $1/V$ as given in equation (2). In other words, a single set of the material properties in (2) can be used to fit all three velocities in experiment 319pfp. Also note that the decay to a constant level, as shown by the position of the dashed lines in Figure 2, depends on time, not slip, a feature of the thermal diffusion distance to the steel in our sample assembly. Another observation that suggests the weakening is due to thermal pressurization comes from comparing L^* for experiment 312pfp with L^* for 319pfp. L^* is larger for 319pfp, although both slid with V=4.8 mm/s, and 319pfp has the higher hydraulic diffusivity. This is what is predicted by equation (2) if the hydraulic diffusivity is much larger than the thermal diffusivity, which is plausibly the case.

Results on material properties

Clearly from the above discussion a more quantitative evaluation of the thermal pressurization weakening in our experiments could be obtained if we knew the values of all the material properties in equations (1) and (2). We have been working on this, but to date we have not been able to come up with a set of values that are compatible with standard tabulated values as well as with equations (1) and (2) and with our observations. We do not regard this as evidence that the

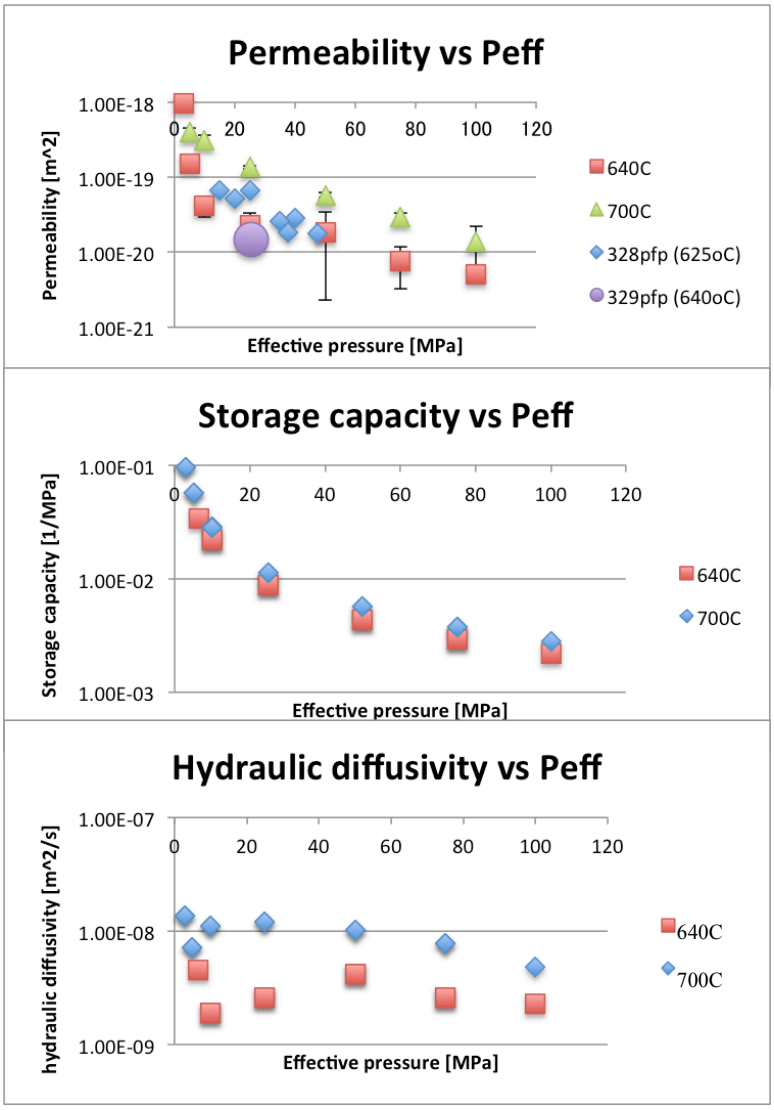

Figure 4. Variation of material properties with effective pressure as measured during this study. The variation of the values is enough that the pore pressure changes during the experiments will be important for details of the behavior. The temperatures that go with the symbols in this figure are those for the heat-treatment prior to the experimental measurements.

weakening is due to some process other than thermal pressurization for the reasons discussed just above. It appears that the difficulties may be due to the dependence of the material properties on the temperature and effective pressure, which change during an experiment. Our FEM program, to date, assumes fixed values of all the material properties, but we have evidence that this is not the case. It is well known that thermal conductivity depends on temperature, a dependence we have not yet taken into account in the FEM model. We have recently collected data that shows that the permeability and the storage capacity depend on the effective pressure and thus so does the hydraulic diffusivity. Figure 4 shows this data.

In addition, the exact values for the thermal conductivity of our rock, especially once it has been thermally cracked, apparently cannot be taken from standard compilations. We show in Figure 5 some data from experiment 319pfp in which we embedded a thermocouple into the sample and ran the very fine wires out to our measuring electronics through the small hole in our high-pressure capillary tubing. This is a very tedious procedure, but provides invaluable data on the temperature reached in the rock and we will attempt this in all our future experiments even though some of our recent experience with broken wire makes it a frustrating experience. The data shown in Figure 5 suggests that the values shown in red of the thermal conductivity K and the density times the heat capacity (the product called Cp in the plot) are better than the nominal tabulated values.

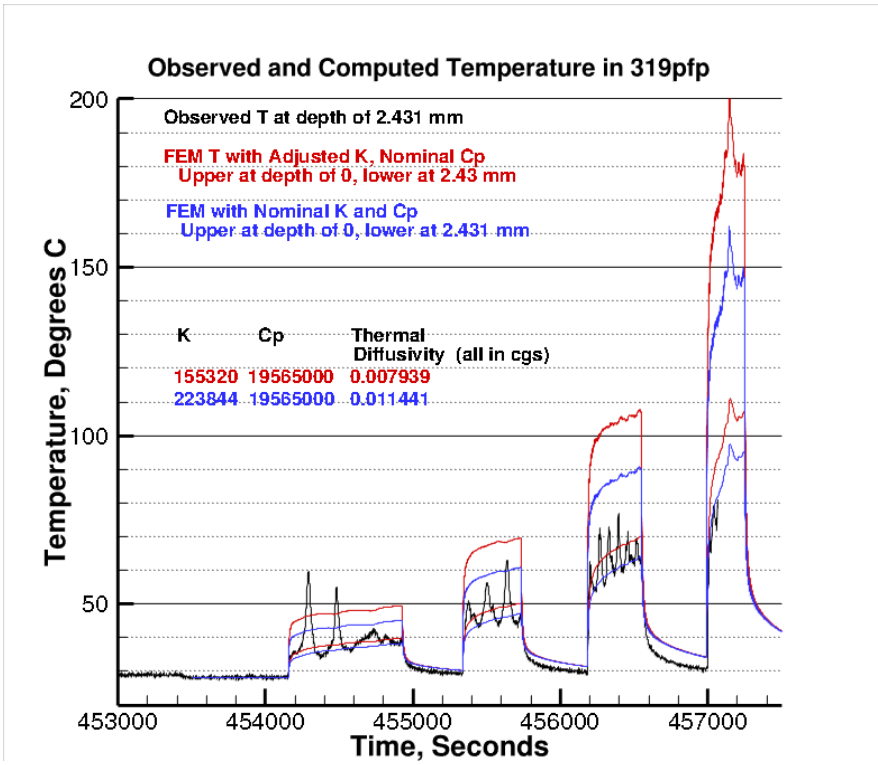

Figure 5. Comparison between observed and FEM computed temperature used to adjust values of thermal conductivity. The red FEM results (lower red lines) match the observed T at depth of 2.43 mm in black better than do the blue (lower blue lines). The elevated Ts occurred when we sequentially raised the slip V to 0.6, 1.2, 2.4, and 4.8 mm/s. The period of the oscillations in observed T correspond to one revolution of the sample ring and show that the normal stress at the circumferential location of the thermocouple depends on the rotational position. This is due to a slight lack of perpendicularity of the sliding surfaces of both halves of the sample to the rotation axis. Our internal LVDT shows that there is a ~6 micron peak-to-peak oscillation in fault-normal displacement with a period of one revolution.

Preliminary FEM results for fluid pressure and temperature

Figure 6 shows results from one of the first computations done using the FEM program in which we compute both thermal and hydraulic diffusion, using frictional heating on the fault as the heat source and thermal expansion of the water in the pores everywhere as the pore-pressure source. There are clearly serious errors in the calculations, especially for the two upper curves in which the rise of the pore pressure on the fault surface is 160 MPa even though the observed drop in the shear stress is only 17 MPa. Although we have added hydraulic diffusion to the FEM program so recently that we have not had time to verify that there are no bugs in it, we suspect that the problem lies in a combination of a) not knowing the material parameters well enough and b) not taking into account the fact that they may vary with time and position during the computation, as the dependence of parameters on the computed field values, such as the dependence on pore pressure shown in Figure 4 illustrates. What is presently frustrating to us with the results of the FEM model is that the values of parameters that we *a priori* took as the best estimates, those for the lower red curves in Figure 5, give the most unreasonable results. One possible problem is that the thermal conductivity that gave the best fit to the thermocouple data for the sample of experiment 319pfp (Figure 5) may not be correct for the sample of experiment 312pfp. They had different heat treatments with resulting permeabilities that differ by a factor of 2.1. If the thermal conductivities also differed by that large a factor then the lower temperature curve in Figure 6 would be the correct one and much of the puzzle would be solved. However, crack density is expected to have a large effect on permeability and a small one on thermal conductivity, so although this could be part of the explanation it is unlikely to be the main solution.

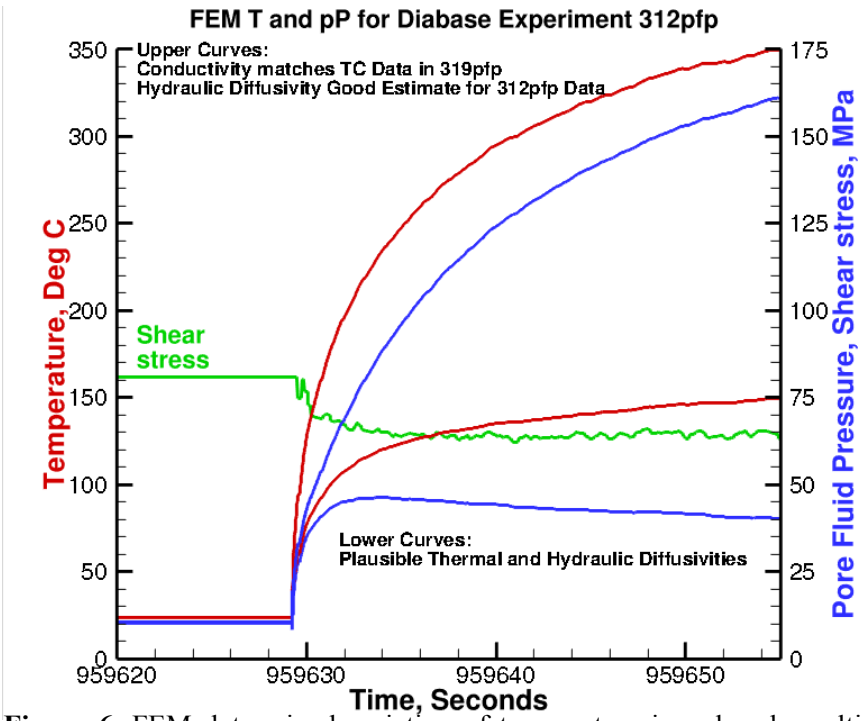

Figure 6. FEM determined variation of temperature in red and resulting pore fluid pressure in blue for two different sets of material properties. Neither set exactly matches the shear stress history in green since the increase in pore pressure is larger than the drop in shear stress (and the coefficient of friction is close to 1.0, namely 0.85 to 0.9 – see equation 1). The results in the upper curves using our *a priori* estimates for thermal conductivity and hydraulic diffusivity are clearly worse than some other plausible values used for the lower curves.

Although we considered not including the bothersome results of Figure 6 in this report, we have included it because it illustrates some of the work we need to do in order to come to a more in-depth understanding of our observed thermal pressurization weakening.

Geophysical implications

All of the weakening mechanisms we have studied have profound implications for the magnitude of stress drops during earthquakes and consequently for the magnitude of strong ground shaking. The manner in which fault strength varies with displacement and slip velocity, as well as the rate at which healing occurs as slip velocity decreases behind the rupture tip, can control the mode of rupture propagation, i.e., as a crack or as a self-healing slip pulse. Furthermore, these data can be important for resolving questions concerning stress levels in the crust. If coseismic friction is low, and the magnitudes of dynamic stress drops are constrained to modest values by seismic data, then the tectonic stress acting on faults must also be modest. We may have a strong crust that is nevertheless able to deform by faulting under modest tectonic stresses if the strength is overcome at earthquake nucleation sites by local stress concentrations and at other places along the fault by dynamic stress concentrations at the rupture front. Thus, understanding high-speed friction is important not only for practical matters related to predicting strong ground-motions and resulting damage, but also for answering major scientific questions receiving considerable attention and funding, e.g., the strength of the San Andreas Fault / the Heat-Flow Paradox, the question that ultimately was responsible for the SAFOD project.

REFERENCES CITED

Andrews, D. J. (2002), A fault constitutive relation accounting for thermal pressurization of pore fluid, *J. Geophys. Res.*, *107*, 12.

Beeler, N. M., T. E. Tullis, and D. L. Goldsby (2008), Constitutive relationships and physical basis of fault strength due to flash-heating, *J. Geophys. Res.*, *113*, B01401, doi:01410.01029/02007JB004988.

Bizzarri, A., and M. Cocco (2006a), A thermal pressurization model for the spontaneous dynamic rupture propagation on a three-dimensional fault: 1. Methodological approach, *J. Geophys. Res.*, *111*, B05303, doi:05310.01029/02005JB003862.

Bizzarri, A., and M. Cocco (2006b), A thermal pressurization model for the spontaneous dynamic rupture propagation on a three-dimensional fault: 2. Traction evolution and dynamic parameters, *J. Geophys. Res.*, *111*, B05304, doi:05310.01029/02005JB003864.

Di Toro, G., D. L. Goldsby, and T. E. Tullis (2004), Friction falls toward zero in quartz rock as slip velocity approaches seismic rates, *Nature*, *427*, 436-439.

Faulkner, D. R., T. M. Mitchell, J. Behnsen, T. Hirose, and T. Shimamoto (2011), Stuck in the mud? Earthquake nucleation and propagation through accretionary forearcs, *Geophys. Res. Lett.*, *38*, L18303, doi:18310.11029/12011GL048552.

Fredrich, J. T., and T.-f. Wong (1986), Micromechanics of thermally induced cracking in three crustal rocks, *J. Geophys. Res.*, *91*, 12,743-712,764.

Goldsby, D. L., and T. E. Tullis (2002), Low frictional strength of quartz rocks at subseismic slip rates, *Geophys. Res. Lett.*, *29*(17), 1844, doi:1810.1029/2002GL015240.

Goldsby, D. L., and T. E. Tullis (2011), Flash heating leads to low strength of crustal rocks at earthquake slip rates, *Science*, *334*, 216-218, DOI: 210.1126/science.1207902.

Kohli, A. H., D. L. Goldsby, G. Hirth, and T. E. Tullis (2011), Flash weakening of serpentinite at near-seismic slip rates, *J. Geophys. Res.*, *116, B03202*, doi:10.1029/2010JB007833.

Lachenbruch, A. H. (1980), Frictional heating, fluid pressure, and the resistance to fault motion, *J. Geophys. Res.*, *85*, 6249-6272.

Lapusta, N., and J. R. Rice (2004a), Earthquake sequences on rate and state faults with strong dynamic weakening, *Eos. Trans. Am. Geophys. Union, Fall Meeting Suppl.*, *85*(47), T22A-05.

Lapusta, N., and J. R. Rice (2004b), Earthquake sequences on rate and state faults with strong dynamic weakening, paper presented at 2004 SCEC Annual Meeting Proceedings and Abstracts, Southern California Earthquake Center, PalmSprings, California, 2004.

Lee, T. C., and P. T. Delaney (1987), Frictional Heating and Pore Pressure Rise Due to a Fault Slip, *Geophysical Journal of the Royal Astronomical Society*, *88*(3), 569-591.

Mase, C. W., and L. Smith (1985), Pore-fluid pressures and frictional heating on a fault surface, *Pure Appl. Geophys.*, *122*, 583-607.

Mase, C. W., and L. Smith (1987), Effects of frictional heating on the thermal hydrologic and mechanical response of a fault, *J. Geophys. Res.*, *92*, 6249-6272.

Noda, H. (2008), Frictional constitutive law at intermediate slip rates accounting for flash heating and thermally activated slip process, *J. Geophys. Res.*, doi:10.1029/2007JB005406.

Noda, H., E. M. Dunham, and J. R. Rice (2009), Earthquake ruptures with thermal weakening and the operation of major faults at low overall stress levels, *J. Geophys. Res.*, *114 (B07302)*, doi:10.1029/2008JB006143.

Noda, H., and N. Lapusta (2010), Three-dimensional earthquake sequence simulations with evolving temperature and pore pressure due to shear heating: Effect of heterogeneous hydraulic diffusivity, *J. Geophys. Res.*, *115*, B12314.

Noda, H., and N. Lapusta (2012), Creeping fault segments can become destructive as a result of dynamic weakening, *Nature*, *493*, 518-521, doi:510.1038/nature11703.

Noda, H., and T. Shimamoto (2005), Thermal pressurization and slip-weakening distance of a fault: An example of the Hanaore fault, southwest Japan, *Bull. Seis. Soc. Am.*, *95*(4), 1224-1233.

Rempel, A. W., and J. R. Rice (2006), Thermal pressurization and onset of melting in fault zones, *Journal of Geophysical Research-Solid Earth*, *111*(B9), B09314, doi:09310.01029/02006JB004314.

Rice, J. R. (2006), Heating and weakening of faults during earthquake slip, *Journal of Geophysical Research-Solid Earth*, *111*(B5), doi:10.1029/2005JB004006.
Rice, J. R., and M. Cocco (2007), Seismic fault rheology and earthquake dynamics, in *The Dynamics of Fault Zones*, edited by M. R. Handy, p. in press, MIT Press, Cambridge, Mass.
Rice, J. R., E. M. Dunham, and H. Noda (2010), Thermo- and hydro-mechanical processes along faults during rapid slip, in *Meso-Scale Shear Physics in Earthquake and Landslide Mechanics*, edited by Y. Hatzor, J. Sulem and I. Vardoulakis, pp. 3-16, CRC Press.
Roig Silva, C., D. L. Goldsby, G. Di Toro, and T. E. Tullis (2004a), The role of silica content in dynamic fault weakening due to gel lubrication, paper presented at 2004 SCEC Annual Meeting Proceedings and Abstracts, Southern California Earthquake Center, Palm Springs, California.
Roig Silva, C., D. L. Goldsby, G. Di Toro, and T. E. Tullis (2004b), The role of silica content in dynamic fault weakening due to gel lubrication, *Eos. Trans. Am. Geophys. Union, Fall Meeting Suppl.*, *85*(47), T21D-07.
Schmitt, S. V., and P. Segall (2009), Thermal pressurization during "slip law" frictional earthquake nucleation, *Poster, 2009 SCEC Annual Meeting*.
Segall, P., and J. R. Rice (2006), Does shear heating of pore fluid contribute to earthquake nucleation?, *Journal of Geophysical Research-Solid Earth*, *111 (B09316)*, doi:10.1029/2005JB004129.
Sibson, R. H. (1973), Interactions between temperature and fluid pressure during earthquake faulting - A mechanism for partial or total stress relief, *Nature*, *243*, 66-68.
Ujiie, K., et al. (2013), Low coseismic shear stress on the Tohoku-Oki megathrust determined from laboratory experiments, *Science*, *342*, 1211-1214.